WAVES IN RANDOM AND COMPLEX MEDIA
2023, VOL. 33, NOS. 5–6, 1346–1365
https://doi.org/10.1080/17455030.2022.2096272

Fourth-order moments analysis for partially coherent electromagnetic beams in random media

Josselin Garnier[a] and Knut Sølna[b]

[a]Centre de Mathématiques Appliquées, Ecole Polytechnique, Institut Polytechnique de Paris, Paris, France;
[b]Department of Mathematics, University of California, Irvine, CA, USA

ABSTRACT

A theory for the characterization of the fourth-order moment of electromagnetic wave beams is presented in the case when the source is partially coherent. A Gaussian–Schell model is used for the partially coherent random source. The white-noise paraxial regime is considered, which holds when the wavelength is much smaller than the correlation radius of the source, the beam radius of the source, and the correlation length of the medium, which are themselves much smaller than the propagation distance. The complex wave amplitude field can then be described by the Itô-Schrödinger equation. This equation gives closed evolution equations for the wave field moments at all orders and here the fourth-order moment equations are considered. The general fourth-order moment equations are solved explicitly in the scintillation regime (when the correlation radius of the source is of the same order as the correlation radius of the medium, but the beam radius is much larger) and the result gives a characterization of the intensity covariance function. The form of the intensity covariance function derives from the solution of the transport equation for the Wigner distribution associated with the second-order wave moment. The fourth-order moment results for polarized waves are used in an application for imaging of partially coherent sources.

ARTICLE HISTORY
Received 19 December 2021
Accepted 20 June 2022

KEYWORDS
Random media; electromagnetic waves; multiple scattering; Schrödinger equation; Gauss–Schell model; scintillation; source imaging

1. Introduction

We consider beam wave propagation in complex media in the situation when we model both the source and the medium as being random. Modeling with a random or complex medium in the context of wave propagation is natural in many situations. In the early foundational work [1,2] and also in Refs. [3,4], a main motivation was propagation through the turbulent atmosphere, but there are many other important applications as well. In cases where one considers propagation through the fluctuating ocean, the earth's crust or through biological tissue, it is also natural and convenient in many cases to model in terms of a random medium [4–6]. In these cases, the medium may be too complex to describe pointwise, but one can hope to be able to describe or model the statistics of the medium fluctuations. The challenge is then to capture the complicated coupling between

CONTACT Knut Sølna ksolna@math.uci.edu

the medium fluctuations and the wave field and to understand how a particular model for the random medium statistics affects the statistics of the wave field which becomes a random field due to random scattering. In this paper, we consider the case of beam waves or paraxial waves in a high-frequency long-range propagation scenario, when the wavelength is much smaller than the correlation radius of the source, the beam radius of the source and the correlation length of the medium, which are themselves much smaller than the propagation distance. In this case, we can approximate the wave field in terms of the solution of the Itô-Schrödinger equation. This equation was analyzed in Ref. [7] and derived from the Helmholtz equation in Ref. [8]. Despite the long history of the theory of waves in random media, a rigorous and explicit description of the fourth-order moment was only obtained in Ref. [9] in the scintillation regime (when the correlation radius of the source is of the same order as the correlation radius of the medium, but the beam radius is much larger). Here we generalize this fourth-order moment theory to the case of polarized waves. This is a deep and quite surprising result in the theory of waves in random media. It states that even though the polarized wave has only partially lost its coherence due to scattering, it behaves from the point of view of the fourth-order moment as if it was a Gaussian field. In some sense, this quasi-Gaussian property explains some of the success or robustness of the theory of waves in random media since the second-order characterization, which in general is relatively easy to obtain, also explains the behavior of fourth-order wave functionals.

Understanding beam propagation through complex media is important because of applications in connection with free-space optical communications, remote sensing and optical imaging. The second-order moments of light beams are analyzed via a Wigner function approach in Refs. [10,11] in order to understand beam resilience to turbulence for certain source beams. The main focus in this paper is on a theory for fourth-order moments which also play an important role in the analysis of applications in imaging and communication. In recent years, there has for instance been a lot of interest in speckle imaging approaches exploiting the speckle memory effect [12,13]. In speckle imaging, one exploits the statistical structure of the speckle and that the speckle pattern may change slowly with illumination in order to carry out imaging through complex media. The speckle pattern corresponds to the structure of the intensity fluctuations, and with the intensity being a quadratic wave field quantity, one then needs to understand fourth-order wave moments to analyze the stability (variance) of the speckle. In Ref. [14], a speckle imaging technique was set forth in a multifrequency context based on an effective spectral decomposition approach with promising experimental results. The analysis of this case then requires results on multifrequency fourth-order wave moments [15]. While the approach in Ref. [14] uses a learned dictionary for computational decomposition of wave intensity, an interesting imaging approach is presented in Ref. [16] where a set of diffractive layers is learned by a deep learning approach for source imaging through a complex section, thus giving an all-optical image reconstruction method.

An important aspect of our modeling in this paper is that we also consider the source as being random. Modeling with a random source may be motivated by the complexity of the source as when one considers emission from a star. A second motivation for understanding and analyzing beam wave propagation from a random source is that such sources have been promoted as being desirable for scintillation reduction when beaming through a complex medium, see Refs. [17–22] and references therein. Scintillation here refers to the situation that the transmitted beam intensity fluctuates rapidly due to scattering over the propagation path. One intuition is that by using a complex source, one gets a better mixing over wave ray paths and a scintillation reduction. Our objective here is to develop an analytic framework where in particular such questions can be analyzed. We consider the Gaussian–Schell model for the source when the source coherence statistics is defined in terms of Gaussian envelopes. This gives rather simple and convenient forms for the wave statistics, but the theory can easily be modified to more general forms for the source statistics. The situation with a partially coherent source, but a homogeneous medium was considered in Ref. [23], while we here consider the case when also the medium is random. Note that we focus on the fourth-order moments, while in Ref. [24] moments of all orders were considered under some simplifying assumptions. The assumption that allows us to get explicit expressions for the fourth-order moments is to assume the scintillation regime, when the correlation radius of the source is of the same order as the correlation radius of the medium, but the beam radius is much larger. Fluctuations of scalar wave intensity were considered in Refs. [25,26] for a beam type propagation when the random medium fluctuations are Gaussian, while we assume Gaussianity for the source, but not for the medium. In Ref. [27], a characterization of intensity fluctuation and how it depends on the regularity of deterministic initial data are presented. Here we consider the case with random initial data with smooth Gaussian statistics.

We remark that there are a number of approaches to model high-order moments of the wave field that are based on perturbative approaches. Indeed, the derivation of such approximations is based on the premise that the waves are only perturbed or affected by the scattering to lower order [3,28,29]. In this paper, we describe an analytic framework that gives a rigorous scaling limit identification of the fourth-order moment in the saturated regime when the incoherent or scattered part of the wave field is as large as or larger than the coherent component. In fact this description also captures the situation when the wave is fully incoherent and the coherent part of the wave energy is essentially fully scattered. The range of validity of this description is discussed in Appendix 3.

We describe next a main result in the paper. We consider the situation when the time-harmonic electric field in the source plane $z = 0$ corresponds to a partially coherent beam and has the form

$$\vec{\boldsymbol{E}}(z=0,\boldsymbol{x}) = \sum_{j=1}^{2} f_j(\boldsymbol{x})\hat{\boldsymbol{e}}_j, \tag{1}$$

where $\hat{\boldsymbol{e}}_1$ and $\hat{\boldsymbol{e}}_2$ are two orthogonal unit vectors in the transverse plane, z is the beam propagation direction and $\boldsymbol{x}$ is the lateral spatial coordinates. The functions f_1, f_2 are zero-mean Gaussian processes with covariance

$$\mathbb{E}\left[f_j\left(\boldsymbol{r}+\frac{\boldsymbol{q}}{2}\right)\overline{f_l}\left(\boldsymbol{r}-\frac{\boldsymbol{q}}{2}\right)\right] = \begin{cases} A_j^2 \exp\left(-\dfrac{|\boldsymbol{r}|^2}{r_o^2} - \dfrac{|\boldsymbol{q}|^2}{4\rho_o^2}\right) & \text{if} \quad j=l, \\ A_jA_l\chi \exp\left(-\dfrac{|\boldsymbol{r}|^2}{r_o^2} - \dfrac{|\boldsymbol{q}|^2}{4\rho_1^2}\right) & \text{if} \quad j\neq l, \end{cases} \tag{2}$$

where the polarization degree $\chi \in [-1,1]$, r_o is the beam radius of the source, ρ_o is the correlation radius of the source and we have $\rho_1 \le \rho_o$. We refer to Ref. [30] for further background on modeling with polarized waves. Consider first the second-order field moment in the form of the mutual coherence function in the white-noise paraxial regime (with the wavelength smaller than the correlation radii of the medium and the beam which are moreover on the scale of the beam radius, which in turn is smaller than the propagation distance, see Appendix 1). As discussed in Section 2, the mutual coherence function of the wave field is in this regime given by

$$\mu_{2,jl}(z,\boldsymbol{r},\boldsymbol{q}) = \mathbb{E}\left[u_j\left(z,\boldsymbol{r}+\frac{\boldsymbol{q}}{2}\right)\overline{u_l}\left(z,\boldsymbol{r}-\frac{\boldsymbol{q}}{2}\right)\right] = \begin{cases} A_j^2\mathcal{H}_{\rho_o}(z,\boldsymbol{r},\boldsymbol{q}) & \text{if} \quad j=l, \\ A_jA_l\chi\mathcal{H}_{\rho_1}(z,\boldsymbol{r},\boldsymbol{q}) & \text{if} \quad j\neq l, \end{cases} \tag{3}$$

where the fundamental second-order lateral scattering function is defined by

$$\mathcal{H}_{\rho_o}(z,\boldsymbol{r},\boldsymbol{q}) = \frac{r_o^2}{4\pi}\int_{\mathbb{R}^2}\exp\left(i\boldsymbol{\zeta}\cdot\boldsymbol{r} - \frac{r_o^2|\boldsymbol{\zeta}|^2}{4} - \frac{|\boldsymbol{\zeta}z/k_o-\boldsymbol{q}|^2}{4\rho_o^2}\right)$$
$$\times\exp\left(\frac{k_o^2}{4}\int_0^z C\left(\frac{\boldsymbol{\zeta}z'}{k_o}-\boldsymbol{q}\right)-C(\boldsymbol{0})\,\mathrm{d}z'\right)\mathrm{d}\boldsymbol{\zeta}, \tag{4}$$

with k_o the central wavenumber and C the covariance function of the medium fluctuations when integrated in the z-dimension (see Equation (18)). The intensity is defined by

$$I(z,\boldsymbol{r}) = \sum_{j=1}^{2}|u_j(z,\boldsymbol{r})|^2, \tag{5}$$

and the mean intensity is then

$$\mathbb{E}\left[I(z,\boldsymbol{r})\right] = (A_1^2+A_2^2)\mathcal{H}_{\rho_o}(z,\boldsymbol{r},\boldsymbol{0}). \tag{6}$$

Consider next the fourth-order field moment in form of the covariance of the intensity. As discussed in Section 3, in the scintillation regime where the wavelength is smaller than the correlation radii of the medium and the beam, which are smaller than the beam radius, which is smaller than the propagation distance, the intensity covariance has the form

$$\mathrm{Cov}\left(I\left(z,\boldsymbol{r}+\frac{\boldsymbol{q}}{2}\right),I\left(z,\boldsymbol{r}-\frac{\boldsymbol{q}}{2}\right)\right) = \left(A_1^4+A_2^4\right)|\mathcal{H}_{\rho_o}(z,\boldsymbol{r},\boldsymbol{q})|^2 + 2A_1^2A_2^2\chi^2|\mathcal{H}_{\rho_1}(z,\boldsymbol{r},\boldsymbol{q})|^2. \tag{7}$$

This representation proves the quasi-Gaussian property that the fourth-order moment (intensity covariance) derives from the second-order moment (the mutual coherence function) as is the case in general for Gaussian random fields. From this description we can identify the intensity decoherence scale and spreading scale and we discuss this explicitly in the strongly scattering case in Section 4. Figure 1 shows the forms of the mean intensity and intensity covariance in this regime and reflects an enhanced spreading and decorrelation due to the random medium. Note that more generally the quasi-Gaussian property provides the basis for analysis of a number of wave propagation challenges and we discuss one such application in Section 4. We remark also that fourth-order moments of the wave fields that are more general than the intensity covariance can be obtained via Proposition A.1 in Appendix 4 and that the quasi-Gaussian property holds for such general moments.

The outline of the paper is as follows. In Section 2, we describe modeling of the partially coherent source in the polarized case and we present the Itô-Schrödinger equation describing wave propagation in the white-noise paraxial regime. In Section 3, we present the fourth-order moment result for the polarized waves. The main result that allows us to

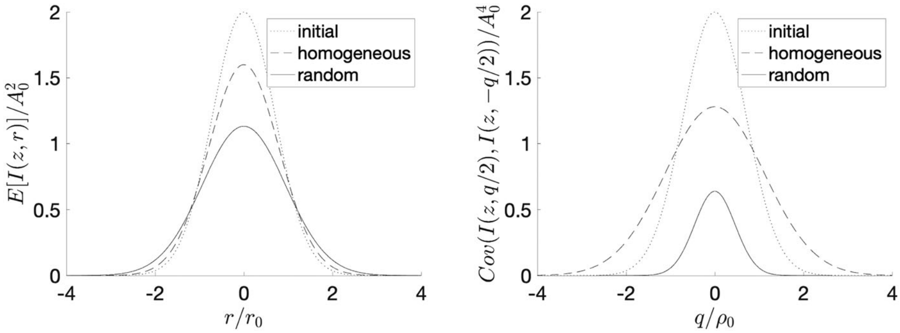

Figure 1. The mean intensity (left) and the intensity covariance (right) when the source is such that $\rho_o = 10\lambda_o, r_o = 100\lambda_o$ (with λ_o the wavelength), $A_1 = A_2 = A_0$ and $\chi = 0$. We compare the profiles of the source (dotted lines) and the profiles of the beam after propagation distance $z = z_o/2$ in the homogeneous medium (dashed lines) and in the random medium with scattering strength $\bar{\gamma}_2 = 5\,10^{-7}\lambda_o^{-1}$ (solid lines). Here $z_o = k_o\rho_o r_o$ is the Rayleigh length of the partially coherent source and $\bar{\gamma}_2$ is defined by Equation (30) and is a measure of the strength of the random fluctuations in the medium.

do this is that the Itô-Schrödinger equations for the polarization modes are dynamically uncoupled, however, statistically coupled. In Section 4, we discuss an application of the theory that we have developed to source imaging (using the intensity covariance function instead of the mutual coherence function as in Ref. [31]). The details of the derivation and also a discussion of the second-order moment or mutual coherence function can be found in the appendices.

2. Electromagnetic waves in the white-noise paraxial regime

We consider propagation of a partially coherent electromagnetic beam waves through a three-dimensional random medium. Maxwell's equations for the three-dimensional electric field $\vec{\boldsymbol{E}}$ and the three-dimensional magnetic field strength $\vec{\boldsymbol{H}}$ are in the time-harmonic case (with frequency ω_o):

$$\nabla \times \vec{\boldsymbol{E}} = -i\omega_o\mu(z,\boldsymbol{x})\vec{\boldsymbol{H}}, \tag{8}$$

$$\nabla \cdot (\epsilon(z,\boldsymbol{x})\vec{\boldsymbol{E}}) = \rho(z,\boldsymbol{x}), \tag{9}$$

$$\nabla \times \vec{\boldsymbol{H}} = \vec{\boldsymbol{J}}^{(s)}(z,\boldsymbol{x}) + i\omega_o\epsilon(z,\boldsymbol{x})\vec{\boldsymbol{E}}, \tag{10}$$

$$\nabla \cdot (\mu(z,\boldsymbol{x})\vec{\boldsymbol{H}}) = 0. \tag{11}$$

The term $\vec{\boldsymbol{J}}^{(s)}$ is a current source term, ϵ is the dielectric permittivity of the medium, and μ is the magnetic permeability of the medium. Note that the equation of continuity of charge $i\omega_o\rho + \nabla \cdot \vec{\boldsymbol{J}}^{(s)} = 0$ is automatically satisfied.

We assume that

- The medium is randomly heterogeneous:

$$\epsilon(z,\boldsymbol{x}) = \epsilon_o\left[1 + m_\epsilon(z,\boldsymbol{x})\right], \tag{12}$$

$$\mu(z,\boldsymbol{x}) = \mu_o\left[1 + m_\mu(z,\boldsymbol{x})\right]. \tag{13}$$

The random processes $m_\epsilon(z, \boldsymbol{x})$ and $m_\mu(z, \boldsymbol{x})$ are bounded, stationary, and zero-mean and they satisfy ergodic (mixing) conditions in z.

- We consider a partially coherent source $\vec{\boldsymbol{f}}(\boldsymbol{x})$, which is a field with Gaussian statistics and mean zero that is localized in the plane $z = 0$. We address the case of a Gauss–Schell model for the source. The source is then $\vec{\boldsymbol{J}}^{(s)}(z, \boldsymbol{x}) = 2\mu_o^{-1/2}\epsilon_0^{1/2}\vec{\boldsymbol{f}}(\boldsymbol{x})\delta(z)$, where $f_3 = 0$ and f_1, f_2 are zero-mean Gaussian processes with covariance

$$\mathbb{E}\left[f_j\left(\boldsymbol{r} + \frac{\boldsymbol{q}}{2}\right)\overline{f_l}\left(\boldsymbol{r} - \frac{\boldsymbol{q}}{2}\right)\right] = \begin{cases} A_j^2 \exp\left(-\frac{|\boldsymbol{r}|^2}{r_o^2} - \frac{|\boldsymbol{q}|^2}{4\rho_o^2}\right) & \text{if} \quad j = l, \\ A_j A_l \chi \exp\left(-\frac{|\boldsymbol{r}|^2}{r_o^2} - \frac{|\boldsymbol{q}|^2}{4\rho_1^2}\right) & \text{if} \quad j \neq l. \end{cases} \tag{14}$$

All parameters are real and positive, with $\chi \in [-1, 1]$. The parameters have to satisfy several constraints to ensure that we deal with a well-defined covariance function:

$$\rho_o \leq r_o, \quad \chi^2\rho_o^{-2} + (1 - \chi^2)r_o^{-2} \leq \rho_1^{-2} \leq \rho_o^{-2}.$$

Here r_o is the radius of the beam and ρ_o is the correlation radius. The special case $\rho_o = r_o, \chi = 0$ corresponds to a coherent source with components $f_j(\boldsymbol{x}) = f_{o,j} \exp(-|\boldsymbol{x}|^2/(2r_o^2))$ where $f_{o,j}, j = 1, 2$ are two independent complex-valued zero-mean Gaussian random variables with variance A_j^2. In the general case with $\rho_o < r_o$, the field is partially coherent and the field components have the form of correlated speckle patterns with speckle spots with typical radius ρ_o and with an overall intensity envelope that is $\exp(-|\boldsymbol{r}|^2/r_o^2)$.

In the white-noise paraxial regime (which holds when the wavelength is much smaller than the correlation radius of the source, the correlation radius of the medium and the beam radius, which are themselves much smaller than the propagation distance), the electric field modulo a range-dependent phase (see Appendix 1) has the form

$$\vec{\boldsymbol{E}}(z, \boldsymbol{x}) = \sum_{j=1}^{2} u_j(z, \boldsymbol{x})\hat{\boldsymbol{e}}_j, \tag{15}$$

where $\hat{\boldsymbol{e}}_1$ and $\hat{\boldsymbol{e}}_2$ are the unit vectors in the transverse plane pointing in the x and y directions and the complex amplitude fields u_j are the solution of the following statistically coupled Itô-Schrödinger equations [8,32,33]:

$$\mathrm{d}u_j(z, \boldsymbol{x}) = \frac{i}{2k_o}\Delta_{\boldsymbol{x}} u_j(z, \boldsymbol{x})\,\mathrm{d}z + \frac{ik_o}{2} u_j(z, \boldsymbol{x}) \circ \mathrm{d}B(z, \boldsymbol{x}), \quad j = 1, 2, \tag{16}$$

with the initial condition in the plane $z = 0$:

$$u_j(z = 0, \boldsymbol{x}) = f_j(\boldsymbol{x}).$$

Here the random process $B(z, \boldsymbol{x})$ is a real-valued Brownian field with a covariance that derives from two-point statistics in the model for the medium fluctuations in (12–13)

$$\mathbb{E}[B(z, \boldsymbol{x})B(z', \boldsymbol{x}')] = \min\{z, z'\}C(\boldsymbol{x} - \boldsymbol{x}'), \tag{17}$$

where

$$C(\boldsymbol{x}) = \int_{\mathbb{R}} \mathbb{E}[(m_\epsilon + m_\mu)(\boldsymbol{x}' + \boldsymbol{x}, z' + z)(m_\epsilon + m_\mu)(\boldsymbol{x}', z')]\,\mathrm{d}z. \tag{18}$$

Note therefore that the evolution equations for the lateral components of the electromagnetic field are driven by the same Brownian field. We remark that $C(\mathbf{0})$ can be interpreted as the product of the variance of the fluctuations of the random medium times its longitudinal correlation radius:

$$C(\mathbf{0}) = \sigma^2 \ell_z$$

for σ the standard deviation of the medium fluctuations: $\sigma^2 = \mathbb{E}[(m_\epsilon + m_\mu)^2(\boldsymbol{x}', z')]$.

The derivation of (16) from the random three-dimensional scalar wave equation is presented in Ref. [8]. Its derivation for the Maxwell's equations (8–11) is presented in Refs. [32,33]. In Equation (16), the symbol ° stands for the Stratonovich stochastic integral [8]. The first- and second-order moments of the wave field solution of (16) have been studied in Refs. [8,32] and recover results derived in Ref. [4]. In view of the centered partial coherent source, we find that the first-order moment of the wave field is zero. The governing equations for the higher order moments can be identified via Itô calculus for Hilbert space valued processes. We find in particular that the second-order moment of the wave field (mutual coherence function) defined by

$$\mu_{2,jl}(z,\boldsymbol{r},\boldsymbol{q}) = \mathbb{E}\left[u_j\left(z, \boldsymbol{r} + \frac{\boldsymbol{q}}{2}\right) \overline{u_l\left(z, \boldsymbol{r} - \frac{\boldsymbol{q}}{2}\right)}\right] \tag{19}$$

satisfies [34]

$$\frac{\partial \mu_{2,jl}}{\partial z} = \frac{i}{k_o} \nabla_{\boldsymbol{r}} \cdot \nabla_{\boldsymbol{q}} \mu_{2,jl} + \frac{k_o^2}{4} U_2\left(\boldsymbol{q}\right) \mu_{2,jl}, \tag{20}$$

with the potential $U_2(\boldsymbol{q}) = C(\boldsymbol{q}) - C(\mathbf{0})$ and the initial condition determined by (14). As shown in Appendix 2, it then follows that the mutual coherence function is given by

$$\mu_{2,jl}(z,\boldsymbol{r},\boldsymbol{q}) = \begin{cases} A_j^2 \mathcal{H}_{\rho_o}(z,\boldsymbol{r},\boldsymbol{q}) & \text{if} \quad j = l, \\ A_j A_l \chi \mathcal{H}_{\rho_1}(z,\boldsymbol{r},\boldsymbol{q}) & \text{if} \quad j \neq l, \end{cases} \tag{21}$$

where $\mathcal{H}_{\rho_o}(z,\boldsymbol{r},\boldsymbol{q})$ is defined by (4).

We next show how our main quantity of interest – the intensity covariance – can be expressed in terms of the mutual coherence function.

3. The intensity covariance for polarized waves

The intensity is defined by (5) and by (3), and its mean is given by (6). The second-order moment of the intensity is

$$\mathbb{E}\left[I\left(z, \boldsymbol{x}_1\right) I\left(z, \boldsymbol{x}_2\right)\right] = \sum_{j,l=1}^{2} \mu_{4,jl}(z, \boldsymbol{x}_1, \boldsymbol{x}_2, \boldsymbol{x}_1, \boldsymbol{x}_2), \tag{22}$$

where the $\mu_{4,jl}$'s are defined by

$$\mu_{4,jl}(z, \boldsymbol{x}_1, \boldsymbol{x}_2, \boldsymbol{y}_1, \boldsymbol{y}_2) = \mathbb{E}\left[u_j(z,\boldsymbol{x}_1)\overline{u_j(z,\boldsymbol{y}_1)} u_l(z,\boldsymbol{x}_2)\overline{u_l(z,\boldsymbol{y}_2)}\right].$$

These moments satisfy Equation (A19) and have the initial conditions:

$$\begin{aligned}
&\mu_{4,jj}(z=0,\boldsymbol{x}_1,\boldsymbol{x}_2,\boldsymbol{y}_1,\boldsymbol{y}_2)\\
&= A_j^4 \exp\left(-\frac{|\boldsymbol{x}_1+\boldsymbol{y}_1|^2}{4r_o^2}-\frac{|\boldsymbol{x}_1-\boldsymbol{y}_1|^2}{4\rho_o^2}-\frac{|\boldsymbol{x}_2+\boldsymbol{y}_2|^2}{4r_o^2}-\frac{|\boldsymbol{x}_2-\boldsymbol{y}_2|^2}{4\rho_o^2}\right)\\
&\quad + A_j^4 \exp\left(-\frac{|\boldsymbol{x}_1+\boldsymbol{y}_2|^2}{4r_o^2}-\frac{|\boldsymbol{x}_1-\boldsymbol{y}_2|^2}{4\rho_o^2}-\frac{|\boldsymbol{x}_2+\boldsymbol{y}_1|^2}{4r_o^2}-\frac{|\boldsymbol{x}_2-\boldsymbol{y}_1|^2}{4\rho_o^2}\right) \qquad (23)
\end{aligned}$$

for $j=1,2$ and

$$\begin{aligned}
&\mu_{4,jl}(z=0,\boldsymbol{x}_1,\boldsymbol{x}_2,\boldsymbol{y}_1,\boldsymbol{y}_2)\\
&= A_j^2A_l^2 \exp\left(-\frac{|\boldsymbol{x}_1+\boldsymbol{y}_1|^2}{4r_o^2}-\frac{|\boldsymbol{x}_1-\boldsymbol{y}_1|^2}{4\rho_o^2}-\frac{|\boldsymbol{x}_2+\boldsymbol{y}_2|^2}{4r_o^2}-\frac{|\boldsymbol{x}_2-\boldsymbol{y}_2|^2}{4\rho_o^2}\right)\\
&\quad + A_j^2A_l^2\chi^2 \exp\left(-\frac{|\boldsymbol{x}_1+\boldsymbol{y}_2|^2}{4r_o^2}-\frac{|\boldsymbol{x}_1-\boldsymbol{y}_2|^2}{4\rho_1^2}-\frac{|\boldsymbol{x}_2+\boldsymbol{y}_1|^2}{4r_o^2}-\frac{|\boldsymbol{x}_2-\boldsymbol{y}_1|^2}{4\rho_1^2}\right) \qquad (24)
\end{aligned}$$

for $j \neq l$.

Consequently, as shown in Appendix 4, in the scintillation regime (which holds in the white-noise paraxial regime when additionally the correlation radius of the source is of the same order as the correlation radius of the medium, but the beam radius is much larger), the second-order moment of the intensity has the form

$$\begin{aligned}
\mathbb{E}\left[I\left(z,\boldsymbol{r}+\frac{\boldsymbol{q}}{2}\right)I\left(z,\boldsymbol{r}-\frac{\boldsymbol{q}}{2}\right)\right] &= \left(A_1^4+A_2^4\right)\left[\mathcal{I}_{\rho_o}(2\boldsymbol{r},\boldsymbol{0})+\mathcal{J}_{\rho_o}(2\boldsymbol{r},\boldsymbol{q})\right]\\
&\quad + 2A_1^2A_2^2\left[\mathcal{I}_{\rho_o}(2\boldsymbol{r},\boldsymbol{0})+\chi^2\mathcal{J}_{\rho_1}(2\boldsymbol{r},\boldsymbol{q})\right], \qquad (25)
\end{aligned}$$

where $\mathcal{I}_{\rho_o}$ and $\mathcal{J}_{\rho_o}$ are defined by (A39) and (A40). This can also be written as

$$\begin{aligned}
\mathbb{E}\left[I\left(z,\boldsymbol{r}+\frac{\boldsymbol{q}}{2}\right)I\left(z,\boldsymbol{r}-\frac{\boldsymbol{q}}{2}\right)\right] &= \left(A_1^4+A_2^4\right)\left[\mathcal{H}_{\rho_o}(z,\boldsymbol{r},\boldsymbol{0})^2+|\mathcal{H}_{\rho_o}(z,\boldsymbol{r},\boldsymbol{q})|^2\right]\\
&\quad + 2A_1^2A_2^2\left[\mathcal{H}_{\rho_o}(z,\boldsymbol{r},\boldsymbol{0})^2+\chi^2|\mathcal{H}_{\rho_1}(z,\boldsymbol{r},\boldsymbol{q})|^2\right] \qquad (26)
\end{aligned}$$

or equivalently (7). This shows that the field satisfies the Gaussian rule for the fourth-order moment in the scintillation regime:

$$\begin{aligned}
&\mathbb{E}\left[I\left(z,\boldsymbol{r}+\frac{\boldsymbol{q}}{2}\right)I\left(z,\boldsymbol{r}-\frac{\boldsymbol{q}}{2}\right)\right]\\
&= \sum_{j,l=1}^{2}\mathbb{E}\left[u_j\left(z,\boldsymbol{r}+\frac{\boldsymbol{q}}{2}\right)\overline{u_j}\left(z,\boldsymbol{r}+\frac{\boldsymbol{q}}{2}\right)\right]\mathbb{E}\left[u_l\left(z,\boldsymbol{r}-\frac{\boldsymbol{q}}{2}\right)\overline{u_l}\left(z,\boldsymbol{r}-\frac{\boldsymbol{q}}{2}\right)\right]\\
&\quad + \sum_{j,l=1}^{2}\mathbb{E}\left[u_j\left(z,\boldsymbol{r}+\frac{\boldsymbol{q}}{2}\right)\overline{u_l}\left(z,\boldsymbol{r}-\frac{\boldsymbol{q}}{2}\right)\right]\mathbb{E}\left[u_l\left(z,\boldsymbol{r}-\frac{\boldsymbol{q}}{2}\right)\overline{u_j}\left(z,\boldsymbol{r}+\frac{\boldsymbol{q}}{2}\right)\right]. \qquad (27)
\end{aligned}$$

The quasi-Gaussianity property and intensity covariance expression that we have just identified are useful in various applications. For instance in applications to imaging based on wave field coherence, the signal-to-noise ratio will in general depend on fourth-order wave field moments [35,36]. These moments can then be related to the mutual coherence function for the wave field via the theory presented in this paper. We discuss next an application to the inverse source problem for partially coherent beam sources in complex media using information that can be extracted from the mean intensity covariance.

4. Estimation of partially coherent electromagnetic sources

We consider the problem of characterizing a partially coherent source. The goal is to determine the parameters of a Gauss–Schell source from the measurements of the intensity after a propagation distance z. Note that here we base the estimate on measurements of intensity only while in for instance in Ref. [31], the estimate is based on coherence of the measurements of the field itself. In Ref. [37], the authors use a cross phase in the source for stable transmission of the coherence pattern in the source field. This then allows for transmission of information. In order to relate the field coherence to coherence in the intensity, the authors use a Gaussian approximation for the field. It follows from the analysis in our paper that such an approximations is valid in the scintillation regime. We remark that in the case with active multifrequency imaging, one can obtain partial phase information from an appropriate illumination strategy and use of a polarization identity [38]. Here we consider passive single-frequency intensity based imaging and no phase information is available.

In the source estimation context considered here, we assume the scintillation regime, moreover, we use the strongly scattering approximation studied in Appendix 3 (which holds when $k_o^2 C(\mathbf{0}) z \gg 1$ and C is smooth). We then find

$$\mathbb{E}\left[I(z,\boldsymbol{r})\right] = (A_1^2 + A_2^2)\frac{r_o^2}{R^2(z;\rho_o)} \exp\left(-\frac{|\boldsymbol{r}|^2}{R^2(z;\rho_o)}\right), \tag{28}$$

where the beam radius is

$$R^2(z;\rho_o) = r_o^2\left(1 + \frac{\bar{\gamma}_2 z^3}{3r_o^2} + \frac{z^2}{k_o^2 r_o^2 \rho_o^2}\right), \tag{29}$$

with

$$\bar{\gamma}_2 = -\frac{1}{4}\Delta_{\boldsymbol{x}} C(\mathbf{0}) \tag{30}$$

being a parameter that governs the strength of random lateral scattering. In the expression (29), the original beam radius is r_o, and the third term in the right-hand side gives the spreading due to diffraction $\mathcal{O}(z)$ in the homogeneous medium case. The second term gives the anomalous spreading $\mathcal{O}(z^{3/2})$ due to random scattering.

The covariance intensity function is

$$\begin{aligned}\mathrm{Cov}\left(I\left(z,\boldsymbol{r}+\frac{\boldsymbol{q}}{2}\right), I\left(z,\boldsymbol{r}-\frac{\boldsymbol{q}}{2}\right)\right) &= \left(A_1^4 + A_2^4\right)\frac{r_o^4}{R(z;\rho_o)^4}\exp\left(-\frac{2|\boldsymbol{r}|^2}{R^2(z;\rho_o)} - \frac{|\boldsymbol{q}|^2}{2\rho^2(z;\rho_o)}\right)\\ &\quad + 2A_1^2A_2^2\chi^2\frac{r_o^4}{R(z;\rho_1)^4}\exp\left(-\frac{2|\boldsymbol{r}|^2}{R^2(z;\rho_1)} - \frac{|\boldsymbol{q}|^2}{2\rho^2(z;\rho_1)}\right),\end{aligned} \tag{31}$$

where the correlation radius of the beam is

$$\rho^2(z;\rho_o) = \rho_o^2\frac{1 + \bar{\gamma}_2 z^3/(3r_o^2) + z^2/(k_o^2\rho_o^2 r_o^2)}{1 + k_o^2\rho_o^2\bar{\gamma}_2 z\left(1 + \bar{\gamma}_2 z^3/(12r_o^2) + z^2/(3k_o^2\rho_o^2 r_o^2)\right)}. \tag{32}$$

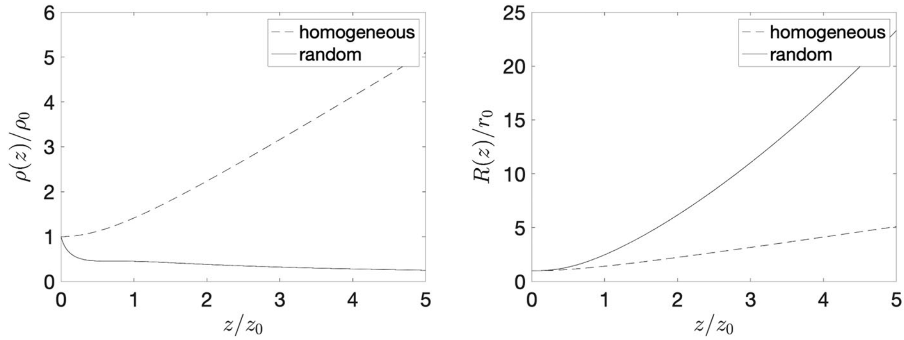

Figure 2. The correlation radius $\rho(z)$ (left) and beam radius $R(z)$ (right) when the source is such that $\rho_o = 10\lambda_o, r_o = 100\lambda_o$ (with λ_o the wavelength), $A_1 = A_2 = A_0$ and $\chi = 0$ as in Figure 1. We compare the functions in the homogeneous medium and in the random medium with scattering strength $\bar{\gamma}_2 = 5\,10^{-7}\lambda_o^{-1}$. Here, $z_o = k_o r_o \rho_o$ is the Rayleigh length of the partially coherent source and $\bar{\gamma}_2$ is defined by Equation (30).

In the homogeneous medium case, we have $\rho(z;\rho_o)/R(z;\rho_o) = \rho_o/r_o$ and the lateral correlation radius increases with the propagation distance while in the random case $\rho(z;\rho_o) = \mathcal{O}(z^{-1/2})$ and the lateral correlation radius decreases with the propagation distance due to random scattering. The correlation radius $\rho(z;\rho_o)$ and beam radius $R(z,\rho_o)$ are plotted in Figure 2. Note that the beam exhibits an anomalous spreading in the random medium, moreover, that the correlation radius is decreasing with depth rather than increasing as in the homogeneous medium. Note also that $\rho \approx \lambda_o$ for deep probing with $z \approx 1/\bar{\gamma}_2$ and that the paraxial approximation is not valid beyond this 'paraxial propagation distance' (also called transport mean free path in the physics literature [39], that is to say, the typical distance after which the direction of light gets lost).

The structure of the intensity covariance in lateral and range coordinates can be used for imaging of the partially coherent source. Here we consider measurements at one range z only. Note that the expressions in (28) and (31) are computed based on averaging with respect to the statistics of both the source and of the medium. We assume that these means can be identified with a high signal-to-noise ratio. This is the case if both the partially coherent source and the medium fluctuate in time and we average the measurements over a time interval that is long compared to the turnover times of the medium and of the source. In cases when the averaging is not efficient or the medium is stationary (time-independent), it may be necessary with some form of filtering to enhance statistical stability [40].

In the statistically stable case with long time averaging at the detector, the observation of the mean intensity and the intensity covariance function make it possible to extract the beam radii $R(z;\rho_o)$, $R(z;\rho_1)$, correlation radii $\rho(z;\rho_o)$, $\rho(z;\rho_1)$ and the intensity amplitude $(A_1^2 + A_2^2)r_o^2$. If $\rho_o \neq \rho_1$, then we can also extract $(A_1^4 + A_2^4)r_o^4$ and $2A_1^2A_2^2\chi^2 r_o^4$. If $\rho_o = \rho_1$, then we can only extract the sum $(A_1^4 + A_2^4 + 2A_1^2A_2^2\chi^2)r_o^4$.

Given the values of z and $\bar{\gamma}_2$, we can then estimate the beam radius r_o of the source, the correlation radii ρ_o and ρ_1, and the total intensity $A_1^2 + A_2^2$. If $\rho_o \neq \rho_1$ we can also extract the polarization degree χ and the ellipticity $e^2 = (A_2^2 - A_1^2)^2/(A_1^2 + A_2^2)^2$. Indeed, if we introduce the three following quantities that can be extracted from data $Y_1 = (a_1^2 + a_2^2)$ and

$Y_2 = a_1^4 + a_2^4$, $Y_3 = 2a_1^2 a_2^2 \chi^2$ with $a_j = A_j r_o$, we have

$$e^2 = \frac{(a_1^2 - a_2^2)^2}{(a_1^2 + a_2^2)^2} = 2\frac{Y_2}{Y_1^2} - 1, \quad \chi^2 = \frac{Y_3}{Y_1^2 - Y_2}. \tag{33}$$

Then, with an estimate of r_o we can identify A_1 and A_2.

The estimation is possible and reliable provided the propagation distance is not too large, i.e. z should not be much larger than $\max((r_o^2/\bar{\gamma}_2)^{1/3}, 1/(\bar{\gamma}_2 k_o^2 \rho_o^2))$, because the statistics of the beam (beam radius and correlation radius) then becomes essentially independent of the initial values r_o and ρ_o as shown in Appendix 3.

5. Conclusions

We have considered time-harmonic electromagnetic wave propagation from partially coherent sources in random media. In many applications of waves, it is of interest to evaluate the fourth-order moment of the wave field. Here we present a theory that allows us to describe such moments and we focus on the specific fourth-order moments corresponding to the intensity covariance. We present here such a description for polarized waves. The results follow from the Itô-Schrödinger equation for the wave field valid in the white-noise paraxial regime. An important aspect of these Itô-Schrödinger equations is that the equations describing the evolutions of the transversely polarized modes are driven by the same Brownian motion, however, such that they are dynamically uncoupled. The explicit expressions for the fourth-order moments are derived in a subsequent scaling regime that we denote the scintillation regime. An important aspect of the fourth-order moment analysis is the proof of the quasi-Gaussian property which means that the fourth-order moments can be obtained from the second-order moments as if the field had Gaussian statistics. We note that this property holds true even if the wave field is partially coherent. We also describe an application to the inverse source problem using information extracted from the observed intensity covariance. We moreover give explicit expressions for the decorrelation and spreading scales deriving from the mutual coherence function for probing through strong clutter, and these scales characterize the statistical structure of the wave field in view of the quasi-Gaussian property (up to fourth order).

Disclosure statement

No potential conflict of interest was reported by the author(s).

Funding

JG was supported by the Agence Nationale pour la Recherche under Grant No. ANR-19-CE46-0007 (project ICCI), and Air Force Office of Scientific Research under grant FA9550-22-1-0176. KS was supported by the Air Force Office of Scientific Research under grant (FA9550-22-1-0176) and the National Science Foundation under grant (DMS-2010046).

References

[1] Tatarskii VI. Waves propagation in a turbulent medium. New York: McGraw-Hill; 1961.

[2] Tatarskii VI. The effects of turbulent atmosphere on wave propagation. U.S. Department of Commerce, TT-68-50464. Springfield; 1971.

[3] Andrews LC, Philipps RL. Laser beam propagation through random media. Bellingham: SPIE Press; 2005.
[4] Ishimaru A. Wave propagation and scattering in random media. Piscataway: IEEE Press; 1997.
[5] Fouque J-P, Garnier J, Papanicolaou G, et al. Wave propagation and time reversal in randomly layered media. New York: Springer; 2007.
[6] Korotkova O. Theoretical statistical optics. Singapore: World Scientific; 2022.
[7] Dawson D, Papanicolaou G. A random wave process. Appl Math Optim. 1984;12(1): 97–114.
[8] Garnier J, Sølna K. Coupled paraxial wave equations in random media in the white-noise regime. Ann Appl Probab. 2009;19(1):318–346.
[9] Garnier J, Sølna K. Fourth-moment analysis for beam propagation in the white-noise paraxial regime. Arch Ration Mech Anal. 2016;220(1):37–81.
[10] Wang J, Wang H, Zhu S, et al. Second-order moments of a twisted Gaussian Schell-model beam in anisotropic turbulence. J Opt Soc Am A. 2018;35(7):1173–1179.
[11] Zhu S, Cai Y, Korotkova O. Propagation factor of a stochastic electromagnetic Gaussian Schell-model beam. Opt Express. 2010;18(12):12587–12598.
[12] Garnier J, Sølna K. Non-invasive imaging through random media. SIAM J Appl Math. 2018;78(6):3296–3315.
[13] Katz O, Small E, Silberberg Y. Looking around corners and through thin turbid layers in real time with scattered incoherent light. Nat Photonics. 2012;6(8):549–553.
[14] Li X, Greenberg JA, Gehm ME. Single-shot multispectral imaging through a thin scatterer. Optica. 2019;6(7):864–871.
[15] Garnier J, Sølna K. Speckle memory effect in the frequency domain and stability in time-reversal experiments, arXiv.2201.05558.
[16] Luo Y, Zhao Y, Li J, et al. Computational imaging without a computer: seeing through random diffusers at the speed of light. eLight. 2022;2(1):4.
[17] Avramov-Zamurovic S, Nelson C, Malek-Madanib R, et al. Polarization-induced reduction in scintillation of optical beams propagating in simulated turbulent atmospheric channels. Waves Random Complex Media. 2014;24(4):452–462.
[18] Avramov-Zamurovic S, Nelson C, Guth S, et al. Flatness parameter influence on scintillation reduction for multi-Gaussian Schell-model beams propagating in turbulent air. Appl Opt. 2016;55(13):3442–3446.
[19] Gbur G. Partially coherent beam propagation in atmospheric turbulence. J Opt Soc Am A. 2014;31(9):2038–2045.
[20] Korotkova O, Gbur G. Applications of optical coherence theory. Prog Opt. 2020;65:43–104.
[21] Voelz D, Fitzhenry K. Pseudo-partially coherent beam for free-space laser communication. Proc SPIE. 2004;5550:218–224.
[22] Wang F, Liu X, Cai Y. Propagation of partially coherent beam in turbulent atmosphere: A review. Prog Electromagn Res. 2015;150:123–143.
[23] Garnier J, Gouédard C, Videau L. Propagation of a partially coherent beam under the interaction of small and large scales. Opt Commun. 2000;176(4–6):281–297.
[24] Fouque J-P, Papanicolaou G, Samuelides Y. Forward and Markov approximation: the strong-intensity-fluctuations regime revisited. Waves Random Media. 1998;8(3):303–314.
[25] Gu Y, Komorowski T. Gaussian fluctuations from random Schrödinger equation. Commun Part Differ Equ. 2021;46(2):201–232.
[26] Komorowski T, Ryzhik L. Fluctuations of solutions to Wigner equation with an Ornstein–Uhlenbeck potential. Discrete Contin Dyn Syst Ser B. 2012;17(3):871–914.
[27] Bal G, Pinaud O. Dynamics of wave scintillation in random media. Commun Partial Differ Equ. 2010;35(7):1176–1235.
[28] Baker G. Gaussian beam weak scintillation: low-order turbulence effects and applicability of the Rytov method. J Opt Soc Am A. 2006;23(2):395–417.
[29] Charnotskii M. Extended Huygens–Fresnel principle and optical waves propagation in turbulence: discussion. J Opt Soc Am A. 2015;32(7):1357–1365.
[30] Born M, Wolf E. Principles of optics. Cambridge: Cambridge University Press; 1999.

[31] Beckus A, Tamasan A, Dogariu A, et al. On the inverse problem of source reconstruction from coherence measurements. J Opt Soc Am A. 2018;35(6):959–968.
[32] Garnier J, Sølna K. Paraxial coupling of electromagnetic waves in random media. SIAM J Multiscale Model Simul. 2009;7(4):1928–1955.
[33] Garnier J, Sølna K. White-noise paraxial approximation for a general random hyperbolic system. SIAM J Multiscale Model Simul. 2015;13(3):1022–1060.
[34] Garnier J, Sølna K. Scintillation in the white-noise paraxial regime. Commun Part Differ Equ. 2014;39(4):626–650.
[35] Borcea L, Garnier J, Papanicolaou G, et al. Enhanced statistical stability in coherent interferometric imaging. Inverse Probl. 2011;27(8):085004.
[36] Garnier J, Papanicolaou G. Passive imaging with ambient noise. Cambridge: Cambridge University Press; 2016.
[37] Liu Y, Chen Y, Wang F, et al. Robust far-field imaging by spatial coherence engineering. Opto-electron adv. 2021;4(12):210027. doi:10.29026/oea.2021.210027.
[38] Moscoso M, Novikov A, Papanicolaou G, et al. Synthetic aperture imaging with intensity-only measurements. IEEE Trans Comput Imaging. 2020;6:87–94.
[39] van Rossum MCW, Nieuwenhuizen TM. Multiple scattering of classical waves: microscopy, mesoscopy, and diffusion. Rev Mod Phys. 1999;71(1):313–371.
[40] Borcea L, Papanicolaou G, Tsogka C. Time and direction of arrival detection and filtering for imaging in strongly scattering random media. Waves Random Complex Media. 2017;27(4):664–689.
[41] Øksendal B. Stochastic differential equations, an introduction with applications. Berlin: Springer; 2007.
[42] Garnier J, Sølna K. Scaling limits for wave pulse transmission and reflection operators. Wave Motion. 2009;46(2):122–143.
[43] Garnier J, Sølna K. Focusing waves through a randomly scattering medium in the white-noise paraxial regime. SIAM J Appl Math. 2017;77(2):500–519.

Appendix 1. The scintillation regime for the electromagnetic waves

We discuss here the white-noise paraxial scaling regime that leads to the Itô-Schrödinger equation in (16). We refer to Ref. [32] for the full derivation. The electromagnetic wave equations have the form (8–11) with the dielectric permittivity ϵ and the magnetic permeability μ of the medium modeled by (12–13). We denote $\vec{\boldsymbol{E}} = (E_j)_{j=1,2,3}$ and $\vec{\boldsymbol{H}} = (H_j)_{j=1,2,3}$. The four-dimensional vector (E_1, H_2, E_2, H_1) then satisfies a closed system as shown in Ref. [32]. Let $c_o = \mu_o^{-1/2}\epsilon_o^{-1/2}$ and $\zeta_o = \mu_o^{1/2}\epsilon_o^{-1/2}$ be the homogeneous propagation speed and impedance, then we introduce the decomposition

$$
\begin{aligned}
E_1(z,\boldsymbol{x}) &= \zeta_o^{1/2}\left(a_1(z,\boldsymbol{x})e^{i(\omega z/c_o)} + b_1(z,\boldsymbol{x})e^{-i(\omega z/c_o)}\right),\\
H_2(z,\boldsymbol{x}) &= \zeta_o^{-(1/2)}\left(a_1(z,\boldsymbol{x})e^{i(\omega z/c_o)} - b_1(z,\boldsymbol{x})e^{-i(\omega z/c_o)}\right),\\
E_2(z,\boldsymbol{x}) &= \zeta_o^{1/2}\left(a_2(z,\boldsymbol{x})e^{i(\omega z/c_o)} + b_2(z,\boldsymbol{x})e^{-i(\omega z/c_o)}\right),\\
H_1(z,\boldsymbol{x}) &= \zeta_o^{-(1/2)}\left(-a_2(z,\boldsymbol{x})e^{i(\omega z/c_o)} + b_2(z,\boldsymbol{x})e^{-i(\omega z/c_o)}\right).
\end{aligned}
$$

Here, $a_j, b_j, j = 1,2$ are coefficients of locally forward and backward (in z) propagating plane waves. In the case of a homogeneous medium with $m_\epsilon \equiv 0, m_\mu \equiv 0$, this gives an exact decomposition into forward and backward plane waves with constant coefficients, while with random medium fluctuations the coefficients a_j and b_j satisfy coupled equations.

Let σ be the standard deviation of the fluctuations of the medium. Moreover, assume that the random fluctuations in the index of refraction are isotropic and denote by ℓ_c the correlation length of the fluctuations, λ_o the carrier wavelength (equal to $2\pi/k_o$, $k_o = \omega_o/c_o$), L the typical propagation distance, ρ_o the correlation radius of the source, and r_o the radius of the initial transverse beam-source. In this framework, the variance $C(\boldsymbol{0})$ of the Brownian field in the Itô-Schrödinger equation (16) is of order $\sigma^2\ell_c$ and the transverse scale of variation of the covariance function $C(\boldsymbol{x})$ in (18) is of order ℓ_c.

We next discuss the scintillation regime in more detail. First, we consider the primary scaling (white-noise paraxial regime) that leads to the Itô-Schrödinger equation (16), when the propagation distance is much larger than the correlation length of the medium, the correlation radius of the source and the beam radius, which are themselves much larger than the wavelength, moreover, the medium fluctuations are small. Explicitly, we assume the primary scaling when

$$\frac{\rho_o}{\ell_c} \sim 1, \quad \frac{r_o}{\ell_c} \sim 1, \quad \frac{L}{\ell_c} \sim \alpha^{-1}, \quad \frac{\lambda_o}{\ell_c} \sim \alpha, \quad \sigma^2 \sim \alpha^3,$$

where α is a small dimensionless parameter. We introduce dimensionless coordinates by

$$\boldsymbol{x} = \ell_c \boldsymbol{x}', \quad z = Lz', \quad k_o = \frac{k_o'}{\ell_c \alpha},$$
$$m_\varepsilon(Lz', \ell_c \boldsymbol{x}') = \alpha^{3/2} m_\varepsilon' \left(z', \boldsymbol{x}'\right), \quad m_\mu(Lz', \ell_c \boldsymbol{x}') = \alpha^{3/2} m_\mu' \left(z', \boldsymbol{x}'\right).$$

We look for the behavior of the coefficient $u_j(z', \boldsymbol{x}') = a_j(z'L, \boldsymbol{x}'\ell_c)$ for long propagation distances of the order of α^{-1}. We obtain a Schrödinger-type equation in which the potential fluctuates in z' on the scale α and is of amplitude $\alpha^{-1/2}$. This diffusion approximation scaling gives the Brownian field and the model (16). As follows from our analysis in Ref. [32], the backward propagating wave components b_j, $j = 1, 2$, are small compared to the forward propagating wave components a_j, $j = 1, 2$, in this forward beam propagation regime. We remark also that the local propagation speed is

$$c = \frac{1}{\sqrt{\mu' \epsilon'}} = c_o \left[1 - \alpha^{3/2} \frac{m_\mu' + m_\epsilon'}{2} + O(\alpha^3) \right],$$

and the local impedance

$$\zeta = \sqrt{\mu'/\epsilon'} = \zeta_o \left[1 + \alpha^{3/2} \frac{m_\mu' - m_\epsilon'}{2} + O(\alpha^3) \right].$$

In view of (18), it then follows that the effective Brownian field is determined by the fluctuations of the local propagation speed, but not by the fluctuations of the local impedance.

In Appendix 4, we address the subsequent scaling regime in which the correlation length of the medium ℓ_c and the correlation radius ρ_o of the source are much smaller than the beam radius r_o of the source; moreover, the medium fluctuations are weak and the beam propagates deep into the medium. We then get the modified scaling picture

$$\frac{\rho_o}{\ell_c} \sim 1, \quad \frac{r_o}{\ell_c} \sim \varepsilon^{-1}, \quad \frac{L}{\ell_c} \sim \alpha^{-1}\varepsilon^{-1}, \quad \frac{\lambda_o}{\ell_c} \sim \alpha, \quad \sigma^2 \sim \alpha^3 \varepsilon, \tag{A1}$$

and we assume $\alpha \ll \varepsilon \ll 1$. This means that the paraxial white-noise limit $\alpha \to 0$ is taken first, and we find

$$2ik_o \, du_j^\varepsilon + \Delta_{\boldsymbol{x}} u_j^\varepsilon \, dz + k_o^2 u_j^\varepsilon \circ dB^\varepsilon(z, \boldsymbol{x}) = 0,$$

where the Brownian field B^ε has covariance C^ε. Then the limit $\varepsilon \to 0$ is applied, corresponding to the scintillation regime. In the scintillation regime (A1), the effective strength $k_o^2 C^\varepsilon(\mathbf{0}) L$ of the Brownian field is of order one since $\sigma^2 \ell_c L/\lambda_o^2 \sim 1$. We also have that $L\lambda_o/r_o^2$ is of order ε. That is, the typical propagation distance is smaller than the Rayleigh length associated to a coherent beam with radius r_o. Here the Rayleigh length corresponds to the distance when the transverse radius of a coherent beam with radius r_o has roughly doubled by diffraction in the homogeneous medium case and it is given by r_o^2/λ_o. The typical propagation distance is, however, of the same order as the Rayleigh length associated to a partially coherent beam with beam radius r_o and correlation radius ρ_o, which is given by $r_o \rho_o/\lambda_o$ [23]. The scintillation regime is, therefore, a regime where diffractive and random effects are both effective and their combination results in non-trivial effects. In this regime we are also able to derive explicit expressions for the fourth-order moment, see Appendix 4.

Appendix 2. The mean polarized-Wigner transform for a partially coherent beam

We discuss here the Wigner transform which is convenient in order to describe second-order field moments. Let $j, l \in \{1,2\}$. The mean Wigner transform is defined by

$$W_{\mathrm{m}}(z, \boldsymbol{r}, \boldsymbol{\xi}) := \int_{\mathbb{R}^2} \exp\left(-i\boldsymbol{\xi}\cdot\boldsymbol{q}\right) \mathbb{E}\left[u_j\left(z, \boldsymbol{r}+\frac{\boldsymbol{q}}{2}\right)\bar{u}_l\left(z, \boldsymbol{r}-\frac{\boldsymbol{q}}{2}\right)\right] \mathrm{d}\boldsymbol{q}. \tag{A2}$$

In view of Equation (20), it satisfies the closed system

$$\frac{\partial W_{\mathrm{m}}}{\partial z} + \frac{1}{k_o}\boldsymbol{\xi}\cdot\nabla_{\boldsymbol{r}} W_{\mathrm{m}} = \frac{k_o^2}{4(2\pi)^2}\int_{\mathbb{R}^2} \hat{C}(\boldsymbol{k})\left[W_{\mathrm{m}}(\boldsymbol{\xi}-\boldsymbol{k}) - W_{\mathrm{m}}(\boldsymbol{\xi})\right]\mathrm{d}\boldsymbol{k}, \tag{A3}$$

starting from $W_{\mathrm{m}}(z=0, \boldsymbol{r}, \boldsymbol{\xi}) = W_{\mathrm{m}0}(\boldsymbol{r}, \boldsymbol{\xi})$, which is the mean Wigner transform of the source (f_j, f_l):

$$W_{\mathrm{m}0}(\boldsymbol{r}, \boldsymbol{\xi}) := \int_{\mathbb{R}^2} \exp\left(-i\boldsymbol{\xi}\cdot\boldsymbol{q}\right) \mathbb{E}\left[f_j\left(\boldsymbol{r}+\frac{\boldsymbol{q}}{2}\right)\bar{f}_l\left(\boldsymbol{r}-\frac{\boldsymbol{q}}{2}\right)\right] \mathrm{d}\boldsymbol{q}.$$

The transport equation (A3) can be solved and we find

$$\begin{aligned} W_{\mathrm{m}}(z, \boldsymbol{r}, \boldsymbol{\xi}) = {} & \frac{1}{(2\pi)^2}\iint_{\mathbb{R}^2\times\mathbb{R}^2} \exp\left(i\boldsymbol{\zeta}\cdot\left(\boldsymbol{r}-\boldsymbol{\xi}\frac{z}{k_o}\right) - i\boldsymbol{\xi}\cdot\boldsymbol{q}\right)\hat{W}_{\mathrm{m}0}(\boldsymbol{\zeta}, \boldsymbol{q}) \\ & \times \exp\left(\frac{k_o^2}{4}\int_0^z C\left(\boldsymbol{q}+\boldsymbol{\zeta}\frac{z'}{k_o}\right) - C(\boldsymbol{0})\,\mathrm{d}z'\right)\mathrm{d}\boldsymbol{\zeta}\,\mathrm{d}\boldsymbol{q}, \end{aligned} \tag{A4}$$

where $\hat{W}_{\mathrm{m}0}$ is defined in terms of the source (f_j, f_l) as

$$\hat{W}_{\mathrm{m}0}(\boldsymbol{\zeta}, \boldsymbol{q}) = \int_{\mathbb{R}^2} \exp\left(-i\boldsymbol{\zeta}\cdot\boldsymbol{r}\right) \mathbb{E}\left[f_j\left(\boldsymbol{r}+\frac{\boldsymbol{q}}{2}\right)\bar{f}_l\left(\boldsymbol{r}-\frac{\boldsymbol{q}}{2}\right)\right] \mathrm{d}\boldsymbol{r}. \tag{A5}$$

The mean Wigner transform gives an equation for the mutual coherence function and we next discuss this in a situation with strong scattering

Appendix 3. The mutual coherence function in the strongly scattering regime

We consider a Gauss–Schell model for the source, which is a field with Gaussian statistics, mean zero, and covariance function (14). By taking the inverse Fourier transform of the mean Wigner transform, we find that the covariance function of the transmitted field has the form (3). We discuss next this mutual coherence function in more detail and to find explicit expressions we assume in the rest of this section that scattering is strong and smooth, in the sense that

$$k_o^2 C(\boldsymbol{0}) z \gg 1, \tag{A6}$$

$$C(\boldsymbol{x}) = C(\boldsymbol{0}) - \bar{\gamma}_2|\boldsymbol{x}|^2 + o(|\boldsymbol{x}|^2). \tag{A7}$$

From (16) written in Itô form [41], it follows that the scattering mean free path ℓ_{mfp} (that is the typical propagation distance over which a coherent wave becomes incoherent) is

$$\ell_{\mathrm{mfp}}^{-1} = \frac{k_o^2 C(\boldsymbol{0})}{8} = \frac{k_o^2\sigma^2\ell_z}{8}. \tag{A8}$$

Thus, in the regime (A6), the propagation distance is large compared to the scattering mean free path. Note moreover that $\bar{\gamma}_2$ can be interpreted as

$$\bar{\gamma}_2 = \frac{\sigma^2\ell_z}{\ell_\perp^2}, \tag{A9}$$

where σ^2 is the variance of medium fluctuations as above, ℓ_z is the longitudinal correlation length of the medium (such that $C(\boldsymbol{0}) = \sigma^2\ell_z$), and $\ell_\perp$ is its transverse correlation radius of the medium defined by

$$\ell_\perp^{-2} = -\frac{\Delta C(\mathbf{0})}{4C(\mathbf{0})}. \tag{A10}$$

If the medium is isotropic (as assumed in Appendix 1), for instance such that $\mathbb{E}[(m_\epsilon + m_\mu)(\mathbf{x}' + z, \mathbf{x}' + z)(m_\epsilon + m_\mu)(\mathbf{x}', z')] = \sigma^2 \exp(-|\mathbf{x}|^2/\ell_c^2 - z^2/\ell_c^2)$, then we have $\ell_z = \sqrt{\pi}\ell_c$ and $\ell_\perp = \ell_c$.

If (A6–A7) hold, then the mean intensity is given by (28). This is found via a Gaussian calculation after inserting (A6) in (4). In this expression we can identify the original beam radius r_o^2, the spreading due to diffraction $z^2/(k_o^2\rho_o^2)$, and the spreading due to random scattering $\bar{\gamma}_2 z^3/3$. The covariance function of the field (or mutual coherence function) is given by

$$\mathbb{E}\left[u_j\left(z, \boldsymbol{r} + \frac{\boldsymbol{q}}{2}\right)\overline{u_j}\left(z, \boldsymbol{r} - \frac{\boldsymbol{q}}{2}\right)\right] = A_j^2 \frac{r_o^2}{R(z;\rho_o)^2} \exp\left(-\frac{|\boldsymbol{r}|^2}{R^2(z;\rho_o)} - \frac{|\boldsymbol{q}|^2}{4\rho^2(z;\rho_o)} + i\theta(z;\rho_o)\boldsymbol{r}\cdot\boldsymbol{q}\right), \tag{A11}$$

where the correlation radius of the beam, $\rho(z;\rho_o)$, is given by (32), the beam radius, $R(z;\rho_o)$, by (29) and

$$\theta(z;\rho_o) = \frac{z/(k_o\rho_o^2) + (k_o\bar{\gamma}_2 z^2/2)}{r_o^2 + (\bar{\gamma}_2 z^3/3) + z^2/(k_o^2\rho_o^2)}. \tag{A12}$$

If the source is coherent $\rho_o = r_o$, then we recover the classical result obtained in Ref. [42], while if the medium is homogeneous and the source is partially coherent $\rho_o < r_o$, then we recover the result obtained in Ref. [23]. Note that if the medium is homogeneous then $1/\sqrt{\theta(z;\rho_o)} \ll \rho(z;\rho_o) \leq R(z;\rho_o)$, as $z \to \infty$, while in the random case $\rho(z;\rho_o) \ll 1/\sqrt{\theta(z;\rho_o)} \ll R(z;\rho_o)$, as $z \to \infty$. In fact in both cases we have $1/\sqrt{\theta} \sim \sqrt{\lambda_o z}$, up to a constant. Thus, the coherent phase modulation is slow relative to the field decorrelation scale for deep probing in the random medium.

For large propagation distance so that the spreading due to the random medium dominates, $z \gg \max((r_o^2/\bar{\gamma}_2)^{1/3}, 1/(\bar{\gamma}_2 k_o^2\rho_o^2))$, we have

$$R(z;\rho_o) \sim \mathcal{A}_{\mathrm{tr}}(z) := \sqrt{\frac{\bar{\gamma}_2 z^3}{3}}, \tag{A13}$$

$$\rho(z;\rho_o) \sim \rho_{\mathrm{tr}}(z) := \frac{1}{k_o\sqrt{\bar{\gamma}_2 z}}, \tag{A14}$$

$$\theta(z;\rho_o) \sim \frac{3k_o}{2z}. \tag{A15}$$

Note that these parameters are independent of the parameters r_o and ρ_o of the partially coherent source, so that information about the source is 'forgotten' in the case of deep probing. We refer to the parameters $\mathcal{A}_{\mathrm{tr}}$, ρ_{tr} as the time reversal aperture and resolution, respectively. We note that we have the Rayleigh resolution relation

$$\rho_{\mathrm{tr}}(L) = \frac{\lambda_o L}{\mathcal{A}_{\mathrm{tr}}(L)}, \tag{A16}$$

where ρ_{tr} corresponds to the refocusing resolution one obtains when a point source emits a wave which is captured on a time reversal mirror at distance L and reemitted (after time reversal) toward the source. Then it will refocus at the original source location with a resolution of the order of the lateral correlation range $\rho_{\mathrm{tr}}(L)$ essentially independently of the actual physical aperture [43]. This can be understood in that the propagator of the transmitted wave decorrelates (laterally) on this scale and the refocused wave is essentially the convolution of the propagator with itself.

We remark that the field correlation radius $\rho(z;\rho_o)$ is important in determining statistical stability. If we average a field quantity over an aperture, then the signal-to-noise ratio will in general depend on the ratio of the aperture to the field correlation radius. We remark finally that we have $\rho_{\mathrm{tr}} \approx \lambda_o$ when $z \approx 1/\bar{\gamma}_2$, which means that the paraxial approximation is not valid beyond this paraxial propagation distance (also called transport mean free path [39]).

Appendix 4. The intensity covariance function

In this appendix, we derive the expression for the intensity covariance function in the scintillation regime. We start by introducing

$$\mu_{4,j_1l_1j_2l_2}(z,\boldsymbol{x}_1,\boldsymbol{x}_2,\boldsymbol{y}_1,\boldsymbol{y}_2) = \mathbb{E}\left[u_{j_1}(z,\boldsymbol{x}_1)\overline{u_{l_1}(z,\boldsymbol{y}_1)}u_{j_2}(z,\boldsymbol{x}_2)\overline{u_{l_2}(z,\boldsymbol{y}_2)}\right]. \tag{A17}$$

We are interested in the second-order moment of the intensity:

$$\mathbb{E}\left[I(z,\boldsymbol{x}_1)I(z,\boldsymbol{x}_2)\right] = \sum_{j_1,j_2=1}^{2} \mu_{4,j_1j_1j_2j_2}(z,\boldsymbol{x}_1,\boldsymbol{x}_2,\boldsymbol{x}_1,\boldsymbol{x}_2). \tag{A18}$$

We find using Equation (16) that the general fourth-order moment $\mu_{4,j_1l_1j_2l_2}$ satisfies the equation

$$\frac{\partial \mu_{4,j_1l_1j_2l_2}}{\partial z} = \frac{i}{2k_o}\left(\Delta_{\boldsymbol{x}_1} + \Delta_{\boldsymbol{x}_2} - \Delta_{\boldsymbol{y}_1} - \Delta_{\boldsymbol{y}_2}\right)\mu_{4,j_1l_1j_2l_2} + \frac{k_o^2}{4}U_4\left(\boldsymbol{x}_1,\boldsymbol{x}_2,\boldsymbol{y}_1,\boldsymbol{y}_2\right)\mu_{4,j_1l_1j_2l_2}, \tag{A19}$$

with the generalized potential

$$\begin{aligned} U_4\left(\boldsymbol{x}_1,\boldsymbol{x}_2,\boldsymbol{y}_1,\boldsymbol{y}_2\right) = {} & C(\boldsymbol{x}_1-\boldsymbol{y}_1) + C(\boldsymbol{x}_2-\boldsymbol{y}_2) + C(\boldsymbol{x}_1-\boldsymbol{y}_2) + C(\boldsymbol{x}_2-\boldsymbol{y}_1) \\ & - C(\boldsymbol{x}_1-\boldsymbol{x}_2) - C(\boldsymbol{y}_1-\boldsymbol{y}_2) - 2C(\boldsymbol{0}), \end{aligned} \tag{A20}$$

and the initial condition:

$$\mu_{4,j_1l_1j_2l_2}(z=0,\boldsymbol{x}_1,\boldsymbol{x}_2,\boldsymbol{y}_1,\boldsymbol{y}_2) = \mathbb{E}\left[f_{j_1}(\boldsymbol{x}_1)\overline{f_{l_1}(\boldsymbol{y}_1)}f_{j_2}(\boldsymbol{x}_2)\overline{f_{l_2}(\boldsymbol{y}_2)}\right].$$

Using the Gaussian property of the source, the initial condition for the fourth-order moment is

$$\begin{aligned} &\mu_{4,j_1l_1j_2l_2}(z=0,\boldsymbol{x}_1,\boldsymbol{x}_2,\boldsymbol{y}_1,\boldsymbol{y}_2) \\ &= \mathbb{E}\left[f_{j_1}(\boldsymbol{x}_1)\overline{f_{l_1}}(\boldsymbol{y}_1)\right]\mathbb{E}\left[f_{j_2}(\boldsymbol{x}_2)\overline{f_{l_2}}(\boldsymbol{y}_2)\right] + \mathbb{E}\left[f_{j_1}(\boldsymbol{x}_1)\overline{f_{l_2}}(\boldsymbol{y}_2)\right]\mathbb{E}\left[f_{j_2}(\boldsymbol{x}_2)\overline{f_{l_1}}(\boldsymbol{y}_1)\right], \end{aligned} \tag{A21}$$

where the covariance function of the source is given by (2).

We parameterize the four points $\boldsymbol{x}_1,\boldsymbol{x}_2,\boldsymbol{y}_1,\boldsymbol{y}_2$ in (A17) in the special way:

$$\boldsymbol{x}_1 = \frac{\boldsymbol{r}_1+\boldsymbol{r}_2+\boldsymbol{q}_1+\boldsymbol{q}_2}{2}, \quad \boldsymbol{y}_1 = \frac{\boldsymbol{r}_1+\boldsymbol{r}_2-\boldsymbol{q}_1-\boldsymbol{q}_2}{2}, \tag{A22}$$

$$\boldsymbol{x}_2 = \frac{\boldsymbol{r}_1-\boldsymbol{r}_2+\boldsymbol{q}_1-\boldsymbol{q}_2}{2}, \quad \boldsymbol{y}_2 = \frac{\boldsymbol{r}_1-\boldsymbol{r}_2-\boldsymbol{q}_1+\boldsymbol{q}_2}{2}. \tag{A23}$$

In particular, $\boldsymbol{r}_1/2$ is the barycenter of the four points $\boldsymbol{x}_1,\boldsymbol{x}_2,\boldsymbol{y}_1,\boldsymbol{y}_2$:

$$\boldsymbol{r}_1 = \frac{\boldsymbol{x}_1+\boldsymbol{x}_2+\boldsymbol{y}_1+\boldsymbol{y}_2}{2}, \quad \boldsymbol{q}_1 = \frac{\boldsymbol{x}_1+\boldsymbol{x}_2-\boldsymbol{y}_1-\boldsymbol{y}_2}{2},$$

$$\boldsymbol{r}_2 = \frac{\boldsymbol{x}_1-\boldsymbol{x}_2+\boldsymbol{y}_1-\boldsymbol{y}_2}{2}, \quad \boldsymbol{q}_2 = \frac{\boldsymbol{x}_1-\boldsymbol{x}_2-\boldsymbol{y}_1+\boldsymbol{y}_2}{2}.$$

We denote by μ the fourth-order moment in these new variables (without writing the dependence on j_1,j_2,l_1,l_2):

$$\mu(z,\boldsymbol{q}_1,\boldsymbol{q}_2,\boldsymbol{r}_1,\boldsymbol{r}_2) = \mu_{4,j_1l_1j_2l_2}(z,\boldsymbol{x}_1,\boldsymbol{x}_2,\boldsymbol{y}_1,\boldsymbol{y}_2), \tag{A24}$$

with $\boldsymbol{x}_1,\boldsymbol{x}_2,\boldsymbol{y}_1,\boldsymbol{y}_2$ given by (A22–A23) in terms of $\boldsymbol{q}_1,\boldsymbol{q}_2,\boldsymbol{r}_1,\boldsymbol{r}_2$.

In the variables $(\boldsymbol{q}_1,\boldsymbol{q}_2,\boldsymbol{r}_1,\boldsymbol{r}_2)$, the function μ satisfies the system:

$$\frac{\partial \mu}{\partial z} = \frac{i}{k_o}\left(\nabla_{\boldsymbol{r}_1}\cdot\nabla_{\boldsymbol{q}_1} + \nabla_{\boldsymbol{r}_2}\cdot\nabla_{\boldsymbol{q}_2}\right)\mu + \frac{k_o^2}{4}U(\boldsymbol{q}_1,\boldsymbol{q}_2,\boldsymbol{r}_1,\boldsymbol{r}_2)\mu, \tag{A25}$$

with the generalized potential

$$\begin{aligned} U(\boldsymbol{q}_1,\boldsymbol{q}_2,\boldsymbol{r}_1,\boldsymbol{r}_2) = {} & C(\boldsymbol{q}_2+\boldsymbol{q}_1) + C(\boldsymbol{q}_2-\boldsymbol{q}_1) + C(\boldsymbol{r}_2+\boldsymbol{q}_1) + C(\boldsymbol{r}_2-\boldsymbol{q}_1) \\ & - C(\boldsymbol{q}_2+\boldsymbol{r}_2) - C(\boldsymbol{q}_2-\boldsymbol{r}_2) - 2C(\boldsymbol{0}). \end{aligned} \tag{A26}$$

Note in particular that the generalized potential does not depend on the barycenter $\boldsymbol{r}_1$, and this comes from the fact that the medium is statistically homogeneous. The Fourier transform (in $\boldsymbol{q}_1,\boldsymbol{q}_2,\boldsymbol{r}_1,$

and $\boldsymbol{r}_2$) of the fourth-order moment is defined by

$$\hat{\mu}(z,\boldsymbol{\xi}_1,\boldsymbol{\xi}_2,\boldsymbol{\zeta}_1,\boldsymbol{\zeta}_2) = \iint_{\mathbb{R}^2\times\mathbb{R}^2} \mu(z,\boldsymbol{q}_1,\boldsymbol{q}_2,\boldsymbol{r}_1,\boldsymbol{r}_2) \times \exp\left(-i\boldsymbol{q}_1\cdot\boldsymbol{\xi}_1 - i\boldsymbol{q}_2\cdot\boldsymbol{\xi}_2 - i\boldsymbol{r}_1\cdot\boldsymbol{\zeta}_1 - i\boldsymbol{r}_2\cdot\boldsymbol{\zeta}_2\right)\,\mathrm{d}\boldsymbol{q}_1\,\mathrm{d}\boldsymbol{q}_2\,\mathrm{d}\boldsymbol{r}_1\,\mathrm{d}\boldsymbol{r}_2. \tag{A27}$$

It satisfies

$$\begin{aligned}\frac{\partial\hat{\mu}}{\partial z} + \frac{i}{k_o}\left(\boldsymbol{\xi}_1\cdot\boldsymbol{\zeta}_1+\boldsymbol{\xi}_2\cdot\boldsymbol{\zeta}_2\right)\hat{\mu} &= \frac{k_o^2}{4(2\pi)^2}\int_{\mathbb{R}^2}\hat{C}(\boldsymbol{k})\big[\hat{\mu}(\boldsymbol{\xi}_1-\boldsymbol{k},\boldsymbol{\xi}_2-\boldsymbol{k},\boldsymbol{\zeta}_1,\boldsymbol{\zeta}_2)\\
&+\hat{\mu}(\boldsymbol{\xi}_1+\boldsymbol{k},\boldsymbol{\xi}_2-\boldsymbol{k},\boldsymbol{\zeta}_1,\boldsymbol{\zeta}_2) - 2\hat{\mu}(\boldsymbol{\xi}_1,\boldsymbol{\xi}_2,\boldsymbol{\zeta}_1,\boldsymbol{\zeta}_2)\\
&+\hat{\mu}(\boldsymbol{\xi}_1+\boldsymbol{k},\boldsymbol{\xi}_2,\boldsymbol{\zeta}_1,\boldsymbol{\zeta}_2-\boldsymbol{k}) + \hat{\mu}(\boldsymbol{\xi}_1-\boldsymbol{k},\boldsymbol{\xi}_2,\boldsymbol{\zeta}_1,\boldsymbol{\zeta}_2-\boldsymbol{k})\\
&-\hat{\mu}(\boldsymbol{\xi}_1,\boldsymbol{\xi}_2-\boldsymbol{k},\boldsymbol{\zeta}_1,\boldsymbol{\zeta}_2-\boldsymbol{k}) - \hat{\mu}(\boldsymbol{\xi}_1,\boldsymbol{\xi}_2+\boldsymbol{k},\boldsymbol{\zeta}_1,\boldsymbol{\zeta}_2-\boldsymbol{k})\big]\,\mathrm{d}\boldsymbol{k}.\end{aligned} \tag{A28}$$

If $j_1 = j_2 = l_2 = l_2 \equiv j \in \{1,2\}$, then the initial condition is

$$\begin{aligned}\hat{\mu}(z=0,\boldsymbol{\xi}_1,\boldsymbol{\xi}_2,\boldsymbol{\zeta}_1,\boldsymbol{\zeta}_2) &= (2\pi)^4A_j^4\phi^1_{\rho_o}(\boldsymbol{\xi}_1)\phi^1_{\rho_o}(\boldsymbol{\xi}_2)\phi^1_{r_o}(\boldsymbol{\zeta}_1)\phi^1_{r_o}(\boldsymbol{\zeta}_2)\\
&+(2\pi)^4A_j^4\phi^1_{\rho_o}(\boldsymbol{\xi}_1)\phi^1_{\rho_o}(\boldsymbol{\zeta}_2)\phi^1_{r_o}(\boldsymbol{\zeta}_1)\phi^1_{r_o}(\boldsymbol{\xi}_2),\end{aligned} \tag{A29}$$

with

$$\phi^1_\rho(\boldsymbol{\xi}) = \frac{\rho^2}{2\pi}\exp\left(-\frac{\rho^2|\boldsymbol{\xi}|^2}{2}\right). \tag{A30}$$

Similar Gaussian expressions hold for the initial condition in the other cases for (j_1,j_2,l_1,l_2), we only address the case $j_1 = j_2 = l_2 = l_2 \equiv j$ in the following.

We cannot solve the problem for the fourth-order moment μ explicitly and consider next a secondary scaling limit where we can identify an explicit solution. We consider the scintillation regime, discussed in more detail in Appendix 1, where the correlation radius of the source is of the same order as the correlation radius of the medium, but the beam radius of the source is much larger:

$$\rho_o \to \rho_o,\quad C(\boldsymbol{x}) \to \varepsilon C(\boldsymbol{x}),\quad r_o \to \frac{r_o}{\varepsilon},\quad z \to \frac{z}{\varepsilon}. \tag{A31}$$

We introduce the rescaled function

$$\tilde{\mu}^\varepsilon(z,\boldsymbol{\xi}_1,\boldsymbol{\xi}_2,\boldsymbol{\zeta}_1,\boldsymbol{\zeta}_2) = \mu\left(\frac{z}{\varepsilon},\boldsymbol{\xi}_1,\boldsymbol{\xi}_2,\boldsymbol{\zeta}_1,\boldsymbol{\zeta}_2\right)\exp\left(i\frac{z}{k_o\varepsilon}(\boldsymbol{\xi}_1\cdot\boldsymbol{\zeta}_1+\boldsymbol{\xi}_2\cdot\boldsymbol{\zeta}_2)\right). \tag{A32}$$

Then the limit $\varepsilon \to 0$ is applied, corresponding to the scintillation regime.

In the scintillation regime, the rescaled function $\tilde{\mu}^\varepsilon$ satisfies the equation with fast phases

$$\begin{aligned}\frac{\partial\tilde{\mu}^\varepsilon}{\partial z} &= \frac{k_o^2}{4(2\pi)^2}\int_{\mathbb{R}^2}\hat{C}(\boldsymbol{k})\big[-2\tilde{\mu}^\varepsilon(\boldsymbol{\xi}_1,\boldsymbol{\xi}_2,\boldsymbol{\zeta}_1,\boldsymbol{\zeta}_2)\\
&+\tilde{\mu}^\varepsilon(\boldsymbol{\xi}_1-\boldsymbol{k},\boldsymbol{\xi}_2-\boldsymbol{k},\boldsymbol{\zeta}_1,\boldsymbol{\zeta}_2)e^{ic_oz/(\varepsilon\omega_o)\boldsymbol{k}\cdot(\boldsymbol{\zeta}_2+\boldsymbol{\zeta}_1)}\\
&+\tilde{\mu}^\varepsilon(\boldsymbol{\xi}_1-\boldsymbol{k},\boldsymbol{\xi}_2,\boldsymbol{\zeta}_1,\boldsymbol{\zeta}_2-\boldsymbol{k})e^{ic_oz/(\varepsilon\omega_o)\boldsymbol{k}\cdot(\boldsymbol{\xi}_2+\boldsymbol{\zeta}_1)}\\
&+\tilde{\mu}^\varepsilon(\boldsymbol{\xi}_1+\boldsymbol{k},\boldsymbol{\xi}_2-\boldsymbol{k},\boldsymbol{\zeta}_1,\boldsymbol{\zeta}_2)e^{ic_oz/(\varepsilon\omega_o)\boldsymbol{k}\cdot(\boldsymbol{\zeta}_2-\boldsymbol{\zeta}_1)}\\
&+\tilde{\mu}^\varepsilon(\boldsymbol{\xi}_1+\boldsymbol{k},\boldsymbol{\xi}_2,\boldsymbol{\zeta}_1,\boldsymbol{\zeta}_2-\boldsymbol{k})e^{ic_oz/(\varepsilon\omega_o)\boldsymbol{k}\cdot(\boldsymbol{\xi}_2-\boldsymbol{\zeta}_1)}\\
&-\tilde{\mu}^\varepsilon(\boldsymbol{\xi}_1,\boldsymbol{\xi}_2-\boldsymbol{k},\boldsymbol{\zeta}_1,\boldsymbol{\zeta}_2-\boldsymbol{k})e^{ic_oz/(\varepsilon\omega_o)(\boldsymbol{k}\cdot(\boldsymbol{\zeta}_2+\boldsymbol{\xi}_2)-|\boldsymbol{k}|^2)}\\
&-\tilde{\mu}^\varepsilon(\boldsymbol{\xi}_1,\boldsymbol{\xi}_2-\boldsymbol{k},\boldsymbol{\zeta}_1,\boldsymbol{\zeta}_2+\boldsymbol{k})e^{ic_oz/(\varepsilon\omega_o)(\boldsymbol{k}\cdot(\boldsymbol{\zeta}_2-\boldsymbol{\xi}_2)+|\boldsymbol{k}|^2)}\big]\,\mathrm{d}\boldsymbol{k},\end{aligned} \tag{A33}$$

starting from

$$\begin{aligned}\tilde{\mu}^\varepsilon(z=0,\boldsymbol{\xi}_1,\boldsymbol{\xi}_2,\boldsymbol{\zeta}_1,\boldsymbol{\zeta}_2) &= (2\pi)^8A_j^4\phi^1_{\rho_o}(\boldsymbol{\xi}_1)\phi^1_{\rho_o}(\boldsymbol{\xi}_2)\phi^\varepsilon_{r_o}(\boldsymbol{\zeta}_1)\phi^\varepsilon_{r_o}(\boldsymbol{\zeta}_2)\\
&+(2\pi)^8A_j^4\phi^1_{\rho_o}(\boldsymbol{\xi}_1)\phi^1_{\rho_o}(\boldsymbol{\zeta}_2)\phi^\varepsilon_{r_o}(\boldsymbol{\zeta}_1)\phi^\varepsilon_{r_o}(\boldsymbol{\xi}_2),\end{aligned} \tag{A34}$$

where ϕ_ρ^ε is defined by

$$\phi_\rho^\varepsilon(\boldsymbol{\xi}) = \frac{\rho^2}{2\pi\varepsilon^2} \exp\left(-\frac{\rho^2}{2\varepsilon^2}|\boldsymbol{\xi}|^2\right). \tag{A35}$$

The following result shows that $\tilde{\mu}^\varepsilon$ exhibits a multi-scale behavior as $\varepsilon \to 0$, with some components evolving at the scale ε and some components evolving on the order one scale [9].

Proposition A.1: *The function $\tilde{\mu}^\varepsilon(z, \boldsymbol{\xi}_1, \boldsymbol{\xi}_2, \boldsymbol{\zeta}_1, \boldsymbol{\zeta}_2)$ can be expanded as*

$$\begin{aligned}
\tilde{\mu}^\varepsilon\left(z, \boldsymbol{\xi}_1, \boldsymbol{\xi}_2, \boldsymbol{\zeta}_1, \boldsymbol{\zeta}_2\right) &= (2\pi)^8 A_j^4 \phi_{r_o}^\varepsilon(\boldsymbol{\zeta}_1)\phi_{r_o}^\varepsilon(\boldsymbol{\zeta}_2) B\left(z, \boldsymbol{\xi}_1, \boldsymbol{\xi}_2, \frac{\boldsymbol{\zeta}_1}{\varepsilon}, \frac{\boldsymbol{\zeta}_2}{\varepsilon}\right) \\
&\quad + (2\pi)^8 A_j^4 \phi_{r_o}^\varepsilon(\boldsymbol{\zeta}_1)\phi_{r_o}^\varepsilon(\boldsymbol{\xi}_2) B\left(z, \boldsymbol{\xi}_1, \boldsymbol{\zeta}_2, \frac{\boldsymbol{\zeta}_1}{\varepsilon}, \frac{\boldsymbol{\xi}_2}{\varepsilon}\right) \\
&\quad + R^\varepsilon(z, \boldsymbol{\xi}_1, \boldsymbol{\xi}_2, \boldsymbol{\zeta}_1, \boldsymbol{\zeta}_2),
\end{aligned} \tag{A36}$$

where

$$\begin{aligned}
B(z, \boldsymbol{\xi}_1, \boldsymbol{\xi}_2, \boldsymbol{\zeta}_1, \boldsymbol{\zeta}_2) &= \frac{1}{(2\pi)^4} \iint_{\mathbb{R}^2\times\mathbb{R}^2} \mathrm{d}\boldsymbol{x}\, \mathrm{d}\boldsymbol{y} \exp\Bigg(-\frac{|\boldsymbol{x}|^2 + |\boldsymbol{y}|^2}{2\rho_o^2} - i\boldsymbol{\xi}_1 \cdot \boldsymbol{x} - i\boldsymbol{\xi}_2 \cdot \boldsymbol{y} \\
&\quad + \frac{k_o^2}{4} \int_0^z C\left(\boldsymbol{x} + \boldsymbol{y} + \frac{z'}{k_o}(\boldsymbol{\zeta}_1 + \boldsymbol{\zeta}_2)\right) + C\left(\boldsymbol{x} - \boldsymbol{y} + \frac{z'}{k_o}(\boldsymbol{\zeta}_1 - \boldsymbol{\zeta}_2)\right) - 2C(\boldsymbol{0})\, \mathrm{d}z'\Bigg),
\end{aligned} \tag{A37}$$

and the function R^ε goes to 0 as $\varepsilon \to 0$.

As a consequence, the second-order moment of the intensity is

$$\mathbb{E}\left[\left|u\left(\frac{z}{\varepsilon}, \frac{\boldsymbol{r}}{\varepsilon} + \frac{\boldsymbol{q}}{2}\right)\right|^2 \left|u\left(\frac{z}{\varepsilon}, \frac{\boldsymbol{r}}{\varepsilon} - \frac{\boldsymbol{q}}{2}\right)\right|^2\right] = A_j^4 \mathcal{I}_{\rho_o}(z, 2\boldsymbol{r}, \boldsymbol{0}) + A_j^4 \mathcal{J}_{\rho_o}(z, 2\boldsymbol{r}, \boldsymbol{q}), \tag{A38}$$

with

$$\begin{aligned}
&\mathcal{I}_{\rho_o}(z, \boldsymbol{r}_1, \boldsymbol{r}_2) \\
&= \iint_{\mathbb{R}^2\times\mathbb{R}^2} \mathrm{d}\boldsymbol{\xi}_1\, \mathrm{d}\boldsymbol{\xi}_2\, \mathrm{d}\boldsymbol{\zeta}_1\, \mathrm{d}\boldsymbol{\zeta}_2 \phi_{r_o}^1(\boldsymbol{\zeta}_1)\phi_{r_o}^1(\boldsymbol{\zeta}_2) B(z, \boldsymbol{\xi}_1, \boldsymbol{\xi}_2, \boldsymbol{\zeta}_1, \boldsymbol{\zeta}_2) \\
&\quad \times \exp\left(-i\frac{z}{k_o}(\boldsymbol{\xi}_1 \cdot \boldsymbol{\zeta}_1 + \boldsymbol{\xi}_2 \cdot \boldsymbol{\zeta}_2) + i\boldsymbol{\zeta}_1 \cdot \boldsymbol{r}_1 + i\boldsymbol{\zeta}_2 \cdot \boldsymbol{r}_2\right) \\
&= \left(\int_{\mathbb{R}^2} \phi_{r_o/\sqrt{2}}^1(\boldsymbol{\zeta}) \exp\left(i\boldsymbol{\zeta} \cdot \frac{\boldsymbol{r}_1 + \boldsymbol{r}_2}{2} + \frac{k_o^2}{4} \int_0^z C\left(\frac{\boldsymbol{\zeta} z'}{k_o}\right) - C(\boldsymbol{0})\, \mathrm{d}z' - \frac{|\boldsymbol{\zeta}|^2 z^2}{4k_o^2\rho_o^2}\right) \mathrm{d}\boldsymbol{\zeta}\right) \\
&\quad \times \left(\int_{\mathbb{R}^2} \phi_{r_o/\sqrt{2}}^1(\boldsymbol{\zeta}) \exp\left(i\boldsymbol{\zeta} \cdot \frac{\boldsymbol{r}_1 - \boldsymbol{r}_2}{2} + \frac{k_o^2}{4} \int_0^z C\left(\frac{\boldsymbol{\zeta} z'}{k_o}\right) - C(\boldsymbol{0})\, \mathrm{d}z' - \frac{|\boldsymbol{\zeta}|^2 z^2}{4k_o^2\rho_o^2}\right) \mathrm{d}\boldsymbol{\zeta}\right) \\
&= \mathcal{H}_{\rho_o}\left(z, \frac{\boldsymbol{r}_1 + \boldsymbol{r}_2}{2}, \boldsymbol{0}\right) \mathcal{H}_{\rho_o}\left(z, \frac{\boldsymbol{r}_1 - \boldsymbol{r}_2}{2}, \boldsymbol{0}\right)
\end{aligned} \tag{A39}$$

and

$$\begin{aligned}
&\mathcal{J}_{\rho_o}(z, \boldsymbol{r}_1, \boldsymbol{r}_2) \\
&= \iint_{\mathbb{R}^2\times\mathbb{R}^2} \mathrm{d}\boldsymbol{\xi}_1\, \mathrm{d}\boldsymbol{\xi}_2\, \mathrm{d}\boldsymbol{\zeta}_1\, \mathrm{d}\boldsymbol{\zeta}_2 \phi_{r_o}^1(\boldsymbol{\zeta}_1)\phi_{r_o}^1(\boldsymbol{\xi}_2) B(z, \boldsymbol{\xi}_1, \boldsymbol{\zeta}_2, \boldsymbol{\zeta}_1, \boldsymbol{\xi}_2) \\
&\quad \times \exp\left(-i\frac{z}{k_o}(\boldsymbol{\xi}_1 \cdot \boldsymbol{\zeta}_1 + \boldsymbol{\xi}_2 \cdot \boldsymbol{\zeta}_2) + i\boldsymbol{\zeta}_1 \cdot \boldsymbol{r}_1 + i\boldsymbol{\zeta}_2 \cdot \boldsymbol{r}_2\right)
\end{aligned}$$

$$= \left| \int_{\mathbb{R}^2} \phi^1_{r_o/\sqrt{2}}(\boldsymbol{\zeta}) \exp\left(i\boldsymbol{\zeta} \cdot \frac{\boldsymbol{r}_1}{2} + \frac{k_o^2}{4} \int_0^z C\left(\frac{\boldsymbol{\zeta} z'}{k_o} - \boldsymbol{r}_2 \right) - C(\boldsymbol{0})\, \mathrm{d}z' - \frac{|(\boldsymbol{\zeta} z/k_o) - \boldsymbol{r}_2|^2}{4\rho_o^2} \right) \mathrm{d}\boldsymbol{\zeta} \right|^2$$

$$= \left| \mathcal{H}_{\rho_o}\left(z, \frac{\boldsymbol{r}_1}{2}, \boldsymbol{r}_2 \right) \right|^2, \tag{A40}$$

where $\mathcal{H}_{\rho_o}$ is defined by (4). We finally remark that for far away points, the second-order moment of the intensity is

$$\mathbb{E}\left[\left| u\left(\frac{z}{\varepsilon}, \frac{\boldsymbol{r}}{\varepsilon} + \frac{\boldsymbol{q}}{2\varepsilon} \right) \right|^2 \left| u\left(\frac{z}{\varepsilon}, \frac{\boldsymbol{r}}{\varepsilon} - \frac{\boldsymbol{q}}{2\varepsilon} \right) \right|^2 \right] = \left(A_1^2 + A_2^2 \right)^2 \mathcal{I}_{\rho_o}(z, 2\boldsymbol{r}, \boldsymbol{q})$$

$$= \left(A_1^2 + A_2^2 \right)^2 \mathcal{H}_{\rho_o}\left(z, \boldsymbol{r} + \frac{\boldsymbol{q}}{2}, \boldsymbol{0} \right) \mathcal{H}_{\rho_o}\left(z, \boldsymbol{r} - \frac{\boldsymbol{q}}{2}, \boldsymbol{0} \right)$$

$$= \mathbb{E}\left[\left| u\left(\frac{z}{\varepsilon}, \frac{\boldsymbol{r}}{\varepsilon} + \frac{\boldsymbol{q}}{2\varepsilon} \right) \right|^2 \right] \mathbb{E}\left[\left| u\left(\frac{z}{\varepsilon}, \frac{\boldsymbol{r}}{\varepsilon} - \frac{\boldsymbol{q}}{2\varepsilon} \right) \right|^2 \right],$$

so that the intensities then indeed are uncorrelated.